Research Paper

Intranetwork and internetwork connectivity in patients with Alzheimer disease and the association with cerebrospinal fluid biomarker levels

Marina Weiler, PhD; Brunno Machado de Campos, PhD; Camila Vieira de Ligo Teixeira, MS; Raphael Fernandes Casseb, MS; Ana Flávia Mac Knight Carletti-Cassani, BSc; Jéssica Elias Vicentini, MS; Thamires Naela Cardoso Magalhães, MS; Leda Leme Talib, PhD; Orestes Vicente Forlenza, MD, PhD; Marcio Luiz Figueredo Balthazar, MD, PhD

Early-released on Apr. 4, 2017; subject to revision

Background: In the last decade, many studies have reported abnormal connectivity within the default mode network (DMN) in patients with Alzheimer disease. Few studies, however, have investigated other networks and their association with pathophysiological proteins obtained from cerebrospinal fluid (CSF). **Methods:** We performed 3 T imaging in patients with mild Alzheimer disease, patients with amnestic mild cognitive impairment (aMCI) and healthy controls, and we collected CSF samples from the patients with aMCI and mild Alzheimer disease. We analyzed 57 regions from 8 networks. Additionally, we performed correlation tests to investigate possible associations between the networks' functional connectivity and the protein levels obtained from the CSF of patients with aMCI and Alzheimer disease. **Results:** Our sample included 41 patients with Alzheimer disease, 35 with aMCI and 48 controls. We found that the main connectivity abnormalities in those with Alzheimer disease occurred between the DMN and task-positive networks: these patients presented not only a decreased anticorrelation between some regions, but also an inversion of the correlation signal (positive correlation instead of anticorrelation). Those with aMCI did not present statistically different connectivity from patients with Alzheimer disease or controls. Abnormal levels of CSF proteins were associated with functional disconnectivity between several regions in both the aMCI and mild Alzheimer disease groups, extending well beyond the DMN or temporal areas. **Limitations:** The presented data are cross-sectional in nature, and our findings are dependent on the choice of seed regions used. **Conclusion:** We found that the main functional connectivity abnormalities occur between the DMN and task-positive networks and that the pathological levels of CSF biomarkers correlate with functional connectivity disruption in patients with Alzheimer disease.

Introduction

In the last decade, there has been an increasing number of studies that use functional MRI (fMRI) to explore the resting-state networks (RSNs), among which the default mode network (DMN) is the most studied in the field of Alzheimer disease. Fewer studies, however, have investigated the functional abnormalities of task-positive RSNs. Results showing, for example, disrupted connectivity in the salience (SAL),[1] executive control (ECN)[2] and language networks (LN),[3] among others, show us that the deleterious effects of Alzheimer disease extend well beyond the regions included in the DMN.

Because the pathology substrates are thought to be spatially spread across brain networks,[4] alterations in one network could be associated with alterations in others, affecting their connectivity. Previous studies have found, for example, disrupted connections between the SAL and ECN[5] and between visuospatial (VSN) and frontoparietal networks[6] in patients with Alzheimer disease. Even individuals at risk for Alzheimer disease (i.e., those with amnestic mild cognitive impairment [aMCI]) have been shown to have disruptions between the SAL and both the ECN and DMN[1] as well as between the dorsal attention (DAN) and sensorimotor networks.[7] Moreover, intercorrelations

Correspondence to: M. Weiler, Neuroimaging Laboratory, Hospital de Clínicas da Unicamp Rua Vital Brasil, 251 Cidade Universitária Zeferino Vaz, Campinas – SP – Brasil; weiler_marina@yahoo.com.br

Submitted Sept. 26, 2016; Revised Nov. 30, 2016; Revised Jan. 10, 2017; Accepted Feb. 25, 2017

DOI: 10.1503/jpn.160190

between the DMN and DAN, between the DMN and sensorimotor network and between the ECN and sensorimotor network have been reported to be reduced with increasing Alzheimer disease severity.[8]

The spatial distribution of the DMN has a striking overlap with the burden of amyloid β ($A\beta_{1–42}$)-pathology in patients with Alzheimer disease,[9] which has been suggested to be a possible explanation for the connectivity disruption involving this network. The link between Aβ burden and disconnectivity of the DMN, for example, has been demonstrated to be true, as detected with Pittsburgh compound B positron emission tomography (PiB-PET) studies in healthy elderly individuals presenting high loads of Aβ pathology.[10] Another widely known pathophysiological feature of Alzheimer disease, however, is the presence of neurofibrillary tangles composed of hyperphosphorylated τ protein (phospho-τ), which may also affect the connectivity of RSNs. As far as we know, however, no studies have investigated the association between the pathophysiological factors of Alzheimer disease obtained from cerebrospinal fluid (CSF) and connectivity between RSNs. Thus, in the present study we investigated connectivity alterations within RSNs, connectivity alterations between RSNs, and possible associations between pathophysiological features of Alzheimer disease extracted from CSF and intra- and internetwork functional connectivity in patients with Alzheimer disease and aMCI.

Methods

Participants

We recruited patients with mild Alzheimer disease, patients with aMCI and healthy controls for participation in our study. To be included in the Alzheimer disease group, patients had to fulfil the standards of the National Institute on Aging–Alzheimer's Association (NIA-AA),[11] and have a Clinical Dementia Rating Scale (CDR)[12] score of 1. Alzheimer disease was diagnosed with the help of MRI.

To be included in the aMCI group, patients had to fulfill the standards of the NIA-AA[13] and have a CDR score of 0.5 with an obligatory memory score of 0.5. We included only those with positive neuroimaging and/or CSF biomarkers. Hippocampal volume was one of the selection criteria for patients with aMCI to enter the study: we used FreeSurfer (https://surfer.nmr.mgh.harvard.edu) for cortical surface reconstruction and anatomic segmentation of the brain MRI scans and included only those whose total hippocampal volume was 20% below the mean volume of the control group (either right or left hippocampus) owing to the higher risk of conversion to Alzheimer disease.[14]

Participants in the control group had to be free of neurologic and psychiatric disorders, have no abnormalities on their structural images and have a CDR score of zero.

Additional exclusion criteria for all participants were history of other neurologic/psychiatric diseases or head injury with loss of consciousness, drug or alcohol addiction, a Hachinski ischemic score[15] above 4 and a Fazekas Scale score[16] above 1. The Medical Research Ethics Committee of the University of Campinas (UNICAMP) approved our study, and we obtained written informed consent from all participants (or from their responsible guardians if the participants were incapable of consenting) before study initiation.

Cerebrospinal fluid sample

We obtained CSF biomarker samples from 27 of the patients with aMCI and 19 of those with Alzheimer disease. The samples were centrifuged at 800*g* for 10 minutes to remove cells and stored at –80° C until protein analysis. We measured $A\beta_{1–42}$, total τ and phospho-τ using the Luminex xMAP platform (Inno-Bia Alzbio3 immunoassay reagents, Innogenetics); cut-off values were chosen based on previous research.[17]

Neuropsychological assessment

Experienced neuropsychologists (A.F.C.-C. and J.E.V.) who were blinded to the MRI data performed the neuropsychological evaluations.

Data acquisition

All MRI scans were acquired using a 3.0 T MRI Philips Achieva scanner. From each participant we obtained a sagittal high-resolution T_1-weighted image with isotropic voxels of 1 mm^3, repetition time (TR) 7 ms, echo time (TE) 3.2 ms, field of view (FOV) 240 × 240 mm and 180 slices; and a functional echo planar image acquisition with TR 2000 ms, TE 30 ms, FOV 240 × 240, isotropic voxels set to 3 mm^3 and no gap with a total scan time of 6 minutes, resulting in 180 dynamics (full brain volumes) with 40 axial slices each. All participants were instructed to keep their eyes closed, to relax, to move as little as possible, and to avoid falling asleep. The MRI procedure lasted 30 minutes.

Functional connectivity analysis

Functional MRI preprocessing and identification of RSNs
We performed the resting-state functional connectivity preprocessing and analysis using an in-house toolbox (UF^2C; www.lni.hc.unicamp.br/app/uf^2c)[18] that runs within the MATLAB platform (2014b, The MathWorks) with SPM12. The image preprocessing routines were based on functional image realignment using the least squares approach with rigid body transformation according to 6 parameters (3 translational and 3 rotational). Because the images were not resliced at this point to avoid redundant interpolation procedures, we used the estimated parameters in the time series regression (described later in this section). The T_1-weighted image was coregistered to the functional mean image (resliced representative functional volume) and segmented into grey matter, white matter and CSF. Subsequently, both the functional and T_1-weighted images were normalized to Montreal Neurological Institute (MNI) space (MNI-152). The functional images were smoothed (3-dimensional spatial Gaussian filter with a 6 × 6 × 6 mm^3 full-width at half-maximum kernel), filtered (band-pass filter 0.008–0.1 Hz) to avoid physiologic confounders,

and regressed for the 6 movement parameters (estimated on the realign step) and for white matter and CSF global signals. Finally, we removed possible remaining linear trends of the time series.

Because it has recently been reported that submillimetre head motion during data scanning can have a substantial impact on some measurements of resting-state fMRI,[19] some participants were excluded from the analysis. No participants exceeded 3 mm of absolute rotation or translation or a maximum spin larger than 3°. We evaluated group differences in head motion among the groups to ensure there were no significant differences in maximum head motion and framewise displacement.

Instead of applying anatomic parcellation as seen in previous studies, we obtained regions of interest (ROIs) from a functional atlas[20] (http://findlab.stanford.edu/functional_ROIs.html). We used a total of 57 ROIs in 8 functional networks: the anterior and posterior SAL, the dorsal and ventral DMN, the left and right ECN, the LN, and the VSN/DAN (Fig. 1, Table 1). The seeds time series extraction criteria were protective against nonfunctionally representative signals. The toolbox uses segmented masks and performs an intraseed voxel covariance analysis, excluding possible outlier voxels from the averages of each seed. This procedure enables connectivity analysis unbiased by atrophic or altered tissues.

Statistical analysis

We performed nonimaging statistical data analysis using SPSS software version 22 (SPSS Inc.). We conducted a χ^2 test to compare the frequency distribution of sex and analyses of variance (ANOVAs) to compare age and years of education among the groups. Nonimaging results were considered to be statistically significant at $p < 0.05$, Bonferroni-corrected for multiple comparisons.

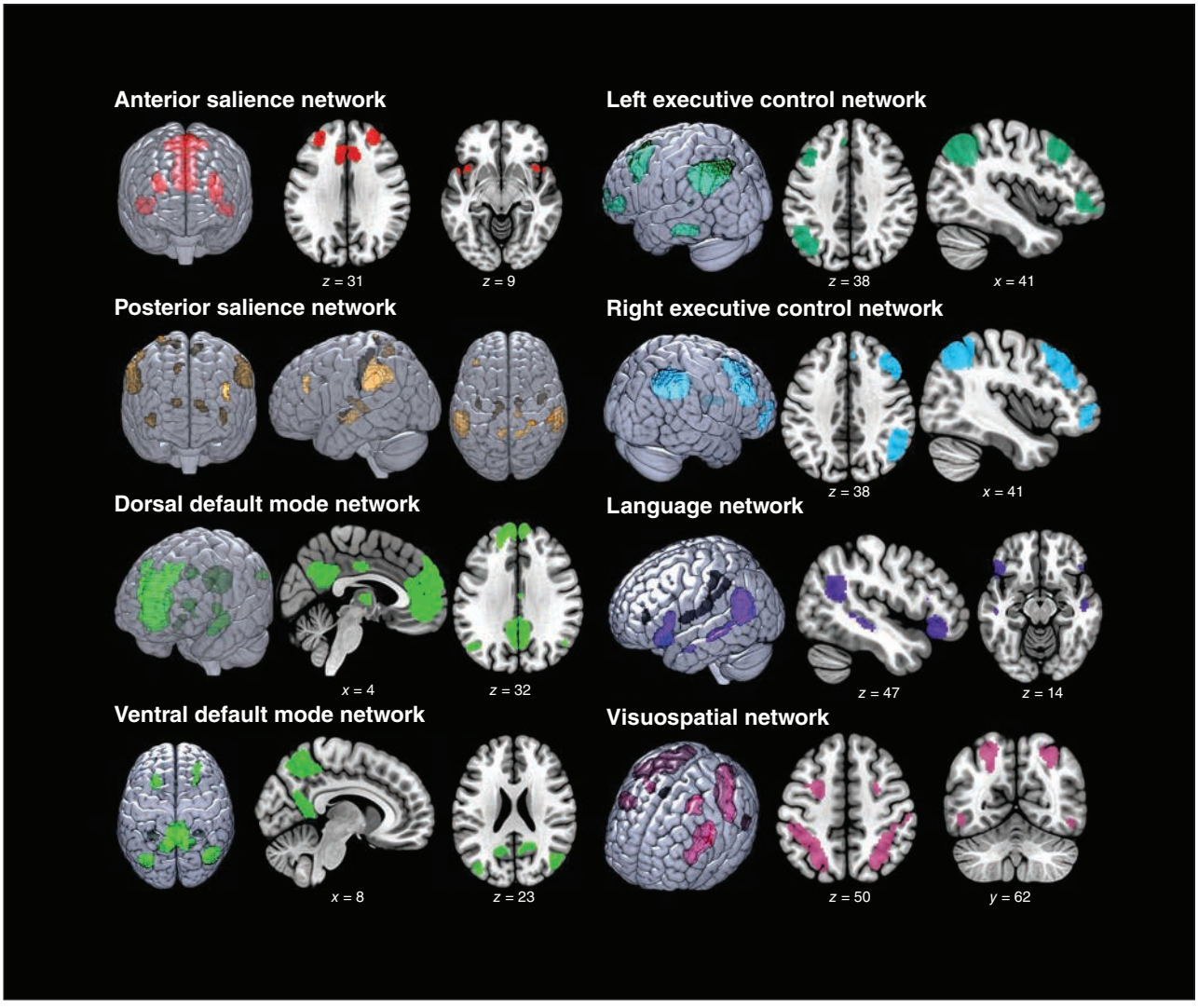

Fig. 1: Spatial maps of the 8 resting-state networks analyzed in this study. Functional regions of interest were obtained from http://findlab.stanford.edu/functional_ROIs.html

Adjacency matrices (ROI × ROI analysis)

The approach used to compare network connectivity among the groups was an ROI-wise analysis. At this step, each ROI of any given network was independently compared with all the other ROIs. We created the cross-correlation matrices by performing Pearson correlation tests (pairwise combination of all 57 ROIs, removing auto [diagonal] and symmetric correlations). These individual correlation matrices were subsequently converted to *z* scores (Fisher *z* transformation) and taken to a group comparison analysis to investigate differences between the control and patient groups. In addition to the comparisons between groups, we also tested for associations between the ROI × ROI functional connectivity and CSF values by performing correlation tests in patients with aMCI and Alzheimer disease. Group comparison and correlation tests between functional connectivity and CSF values were performed in our UF²C toolbox.

For the group comparison analysis, the terms "decreased connectivity" and "increased connectivity" were used to classify the alterations among groups and indicate whether the patients had lower or higher absolute connectivity values (using a group score as the reference). In this sense, "decreased" refers to Pearson correlation values farther away from zero when compared with controls, and "increased" refers to Pearson correlation values closer to zero when compared with controls. The statistical tests, however, were performed with the original values, making sure that comparisons among correlations in opposite directions had been considered accordingly in the statistical analysis. The UF²C toolbox not only shows statistical differences among groups, but also distinctly presents comparisons among positive values and negative values and highlights situations in which the correlation signals are opposite among groups, whereas most fMRI toolboxes exclude negative correlations from the analysis or use absolute values. As 2 networks with negative correlation values are said to be anticorrelated, decreased negative value is equivalent to less anticorrelation, whereas increased negative value is equivalent to more anticorrelation. We considered results for imaging data to be

Table 1 (part 1 of 2): Anatomic location of the 57 regions of interest used to characterize the 8 resting-state networks*

Network	ROI	Anatomic location	MNI reference, *x*, *y*, *z*	ROI size (voxels)
Anterior salience (n1)	r1n1	Left middle frontal gyrus	–30, 46, 8	651
	r2n1	Left insula	–46, 14, –12	305
	r3n1	Anterior cingulate cortex, medial prefrontal cortex	–8, 32, 16	2887
	r4n1	Right middle frontal gyrus	28, 46, 16	470
	r5n1	Right insula	48, 14, –10	319
Posterior salience (n2)	r1n2	Left middle frontal gyrus	–38, 34, 20	93
	r2n2	Left supramarginal gyrus, inferior parietal gyrus	–58, –38, 24	1205
	r3n2	Left precuneus	–4, –50, 56	98
	r4n2	Right middle cingulate cortex	14, –26, 40	56
	r5n2	Right precuneus, superior parietal gyrus	12, –58, 62	133
	r6n2	Right supramarginal gyrus, inferior parietal gyrus	62, –24, 18	1002
	r7n2	Left thalamus	–16, –32, –2	142
	r8n2	Left posterior insula	–36, –10, –14	114
	r9n2	Right thalamus	14, –22, 4	63
	r10n2	Right posterior insula	38, –4, –16	134
Dorsal default mode (n3)	r1n3	Medial prefrontal cortex, anterior cingulate cortex	2, 44, –28	5257
	r2n3	Left angular gyrus	–50, –68, 30	97
	r3n3	Right superior frontal gyrus	22, 40, 40	137
	r4n3	Posterior cingulate cortex, precuneus	–4, –54, 12	1555
	r5n3	Midcingulate cortex	4, –16, 32	114
	r6n3	Right angular gyrus	52, –64, 28	38
	r7n3	Left and right thalamus	–8, –12, –8	220
	r8n3	Left hippocampus	–22, –16, –26	393
	r9n3	Right hippocampus	26, –16, –26	142
Ventral default mode (n4)	r1n4	Left retrosplenial cortex, posterior cingulate cortex	–8, –54, 4	462
	r2n4	Left middle frontal gyrus	–24, 10, 44	405
	r3n4	Left parahipocampal gyrus	–28, –30, –24	134
	r4n4	Left middle occipital gyrus	–40, –82, 22	491
	r5n4	Right retrosplenial cortex, posterior cingulate cortex	14, –46, 0	590
	r6n4	Precuneus	4, –60, 40	1921
	r7n4	Right superior frontal gyrus, middle frontal gyrus	24, 32, 32	399
	r8n4	Right parahipocampal gyrus	30, –32, 24	90
	r9n4	Right angular gyrus, middle occipital gyrus	52, –66, 18	752

significant at $p < 0.05$, false discovery rate (FDR)–corrected for multiplicity.

Results

Demographic and neuropsychological data

This study included 124 participants: 41 patients with mild Alzheimer disease, 35 with aMCI and 48 healthy controls. Table 2 shows the demographic and neuropsychological data of the sample. Groups did not differ in sex or age; however, they differed in years of education, and this variable was included as a confounding factor in the analysis.

Cerebrospinal fluid values

The mean CSF biomarker protein values of the aMCI sample were as follows: total τ 97.1 ± 72.58, phospho-τ 43.57 ± 32.86, $A\beta_{1–42}$ 386.56 ± 173.71 and $A\beta_{1–42}$/phospho-τ 8.09 ± 7.6. The mean values for the Alzheimer disease group were as follows: total τ 170.84 ± 73.95, phospho-τ 54.87 ± 30.69, $A\beta_{1–42}$ 360.86 ± 100.88 and $A\beta_{1–42}$/phospho-τ 7.18 ± 4.91. There were no signicant differences in total τ ($p = 0.09$), phospho-τ ($p = 0.47$), $A\beta_{1–42}$ ($p = 0.66$), or $A\beta_{1–42}$/phospho-τ ($p = 0.98$) between the 2 patient groups.

Functional connectivity analysis

Owing to head motion during scanning, 2 controls, 3 patients with aMCI and 5 with mild Alzheimer disease were excluded from the functional connectivity analysis.

Controls versus patients with aMCI

The ROI × ROI analysis demonstrated that patients with aMCI did not present FDR-corrected statistically different results from controls. Uncorrected ($p < 0.001$) results for multiplicity, adjusted for years of education, show that compared with controls patients with aMCI had decreased internetwork functional connectivity between some ROIs of the ventral and dorsal DMN, the posterior SAL and the VSN/DAN. We observed inversion of the correlation signal in ROIs belonging to the ventral and dorsal DMN and the LN. From a network perspective, regions of the DMN were mainly affected, specifically parietal and posterior cingulate regions (Appendix 1, Fig. S1, available at jpn.ca).

Controls versus patients with mild Alzheimer disease

Compared with controls, patients with mild Alzheimer disease had 7 networks with alterations (only the anterior SAL showed no functional connectivity disruption) in the pairwise ROI analysis, adjusted for years of education, that survived to FDR-correction. In total, 19 ROIs linked by 17 connections

Table 1 (part 2 of 2): Anatomic location of the 57 regions of interest used to characterize the 8 resting-state networks*

Network	ROI	Anatomic location	MNI reference, *x*, *y*, *z*	ROI size (voxels)
Language (n5)	r1n5	Left inferior frontal gyrus	–46, 24, –20	652
	r2n5	Left middle temporal gyrus	–52, –4, –24	27
	r3n5	Left middle temporal gyrus, angular gyrus	–50, –26, –14	317
	r4n5	Left middle temporal gyrus, superior temporal gyrus	–56, –54, 4	1420
	r5n5	Right inferior frontal gyrus	46, 28, –16	58
	r6n5	Right middle temporal gyrus, angular gyrus	48, –14, –18	1106
Left executive control (n6)	r1n6	Left middle frontal gyrus, superior frontal gyrus	–48, 18, 28	1501
	r2n6	Left inferior frontal gyrus, orbitofrontal gyrus	–38, 42, –12	437
	r3n6	Left superior parietal gyrus, inferior parietal gyrus, angular gyrus	–50, –64, 28	2110
	r4n6	Left inferior temporal gyrus, middle temporal gyrus	–56, –30, –20	350
	r5n6	Left thalamus	–14, –29, 0	8
Right executive control (n7)	r1n7	Right middle frontal gyrus, superior frontal gyrus	50, 30, 16	2093
	r2n7	Right middle frontal gyrus	44, 46, –14	356
	r3n7	Right inferior parietal gyrus, supramarginal gyrus, angular gyrus	48, –60, 32	1873
	r4n7	Right superior frontal gyrus	6, 34, 38	83
	r5n7	Right caudate	10, –4, 8	188
Visuospatial/dorsal attention (n8)	r1n8	Left middle frontal gyrus, superior frontal gyrus, precentral gyrus	–22, –4, 46	338
	r2n8	Left inferior parietal gyrus	–54, –30, 30	2020
	r3n8	Left frontal operculum, inferior frontal gyrus	–40, 30, 8	1105
	r4n8	Left inferior temporal gyrus	–48, –64, –12	93
	r5n8	Right middle frontal gyrus	28, –2, 48	97
	r6n8	Right inferior parietal gyrus	30, –64, 36	1193
	r7n8	Right frontal operculum, inferior frontal gyrus	50, 12, 16	326
	r8n8	Right inferior temporal gyrus	50, –62, –14	76

MNI = Montreal Neurological Institute; ROI = region of interest.
*Regions of interest obtained from http://findlab.stanford.edu/functional_ROIs.html

showed disrupted functional connectivity in this group relative to the control sample. Patients with mild Alzheimer disease showed an intranetwork positive connectivity decrease (closer to zero) between 2 ROIs of the right ECN (r1n7–r3n7), whereas a decreased internetwork anticorrelation (closer to zero) was found between an ROI belonging to the LN (r1n5) and a region of the ventral DMN (r6n4), between the left ECN (r3n6) and posterior SAL (r5n2), and between the dorsal DMN (r2n3) and the VSN/DAN (r8n8; Fig. 2). We observed increased internetwork positive connectivity (farther away from zero) between the left ECN (r2n6) and 2 regions of the dorsal DMN (r1n3 and r6n3; Fig. 2). An inversion of the correlation signal was found mainly in 3 regions: the first belonging to the VSN/DAN, the second belonging to the left ECN, and the third belonging to the LN (Table 3, Fig. 2), and in all of these connections the correlation signal was negative in controls and positive in patients with Alzheimer disease.

From a network perspective, patients with mild Alzheimer disease showed less anticorrelation between the right ECN and posterior SAL, LN and ventral DMN; a weaker negative correlation between the dorsal DMN and VSN/DAN; and a weaker positive correlation within the right ECN than controls. On the other hand, a stronger positive connectivity was found between the left ECN and dorsal DMN. The inversion of the correlation signal was observed mainly between anteroposterior areas (i.e., between the left inferior frontal area and the posterior cingulate cortex/precuneus) and largely affected the connection between the DMN and VSN/DAN and between the left ECN and the LN, which were anticorrelated in controls and positively correlated in patients with mild Alzheimer disease.

Patients with aMCI versus patients with mild Alzheimer disease

The ROI × ROI analysis showed that patients with aMCI did not present FDR-corrected statistically different results from patients with mild Alzheimer disease. Uncorrected results ($p < 0.001$), adjusted for years of education, showed that compared with patients with aMCI, those with mild Alzheimer disease had decreased internetwork connectivity in between

Table 2: Demographic and neuropsychological characteristics of the study population

	Group; mean ± SD*			*p* value; comparison		
Characteristic	Control, *n* = 48	aMCI, *n* = 35	Alzheimer, *n* = 41	Control v. aMCI	aMCI v. Alzheimer	Control v. Alzheimer
Female sex, no. (%)	33 (69)	23 (65)	26 (63)	—	—	—
Age, yr	68.12 ± 8.78	68.32 ± 6.4	72.21 ± 12.94	> 0.99	0.25	0.16
Education, yr	11.86 ± 5.6	9.05 ± 5.45	7.33 ± 5.3	0.047	0.33	0.001
CDR score	0	0.5	1	—	—	—
MMSE	28.61 ± 1.68	22.94 ± 2.6	19.53 ± 3.82	< 0.001	0.048	< 0.001
Episodic memory tests						
RAVLT encoding	45.02 ± 9.19	28.94 ± 8.44	20.12 ± 6.76	< 0.001	0.003	< 0.001
RAVLT A7	8.64 ± 2.74	3.21 ± 2.09	1 ± 1.37	< 0.001	< 0.001	< 0.001
RAVLT CR-FP	11.34 ± 3.35	5.42 ± 6.06	-2.6 ± 5.1	< 0.001	< 0.001	< 0.001
Working memory/attention tests						
FDS	5.48 ± 1.45	4.53 ± 0.94	3.76 ± 1.4	0.008	0.80	< 0.001
BDS	4.34 ± 1.14	3.36 ± 1.06	2.2 ± 1.5	0.005	0.002	< 0.001
Language tests						
SVF	17.66 ± 4.6	12.65 ± 3.95	9.72 ± 4.79	< 0.001	0.003	< 0.001
FAS	35.5 ± 11.65	27.82 ± 9.9	20.2 ± 12.03	0.015	0.026	< 0.001
BNT	63.36 ± 71.05	49 ± 9.37	38.52 ± 12.5	0.56	0.90	0.039
Executive function tests						
Stroop C,s	50.05 ± 16.14	47.94 ± 13.25	70.4 ± 35.32	> 0.99	< 0.001	< 0.001
Stroop C, errors	0.09 ± 0.03	0.03 ± 0.02	0.52 ± 1.05	> 0.99	0.002	0.001
Stroop I, s	104.02 ± 28.08	130.47 ± 60.11	168.88 ± 90.98	0.27	0.042	0.001
Stroop I, errors	3.3 ± 4.71	6.94 ± 8.9	19.83 ± 18.55	0.85	< 0.001	< 0.001
TMT-A, s	61.18 ± 18.02	91.96 ± 50.45	161.52 ± 114.33	0.18	< 0.001	< 0.001
TMT-B, s	112.24 ± 74.07	141.59 ± 90.2	198.24 ± 133.52	0.60	0.06	0.001
Visuospatial skill tests						
Rey figure copy	41.75 ± 3.15	27.12 ± 10.23	19.16 ± 13.19	0.13	0.91	0.005
Clock drawing (0–10)	9.09 ± 1.61	8.76 ± 1.85	5.48 ± 2.64	0.07	< 0.001	< 0.001
LNI	17.96 ± 1.38	17.94 ± 4.85	14.32 ± 4.31	> 0.99	0.005	< 0.001

aMCI = amnestic mild cognitive impairment; BDS = backward digit span; BNT = Boston naming test; C = congruent; FAS = phonological fluency for letters; FDS = forward digit span; I = incongruent; LNI = Luria's neuropsychological investigation; MMSE = Mini-Mental Status Examination; RAVLT = Rey Auditory Verbal Learning Test; RAVLT A7 = delayed recall of Rey auditory verbal learning test; RAVLT RC-FP = Rey auditory verbal learning test true recognition (correct recognition – false positives); Rey = Rey-Osterrieth Complex Figure Test; SD = standard deviation; SVF = semantic verbal fluency; TMT = Trail Making Test.
*Unless indicated otherwise.

the left ECN and the posterior SAL and dorsal DMN. Inversion of the correlation signal was found between the ventral DMN and left ECN and between the VSN/DAN and several ROIs of the DMN (Appendix 1, Fig. S2).

Association between functional connectivity and CSF values

In the aMCI group, the functional connectivity of the following regions showed a positive association with CSF total τ levels: the ventral DMN (r8n4) and the LN (r5n5), the posterior SAL (r1n2) and the VSN/DAN (r3n8), and the VSN/DAN (r3n8) and both the dorsal DMN (r8n3) and the ventral DMN (r3n4). We found a negative correlation between the functional connectivity between the VSN/DAN (r3n8) and the ventral DMN (r2n4). Phospho-τ was positively associated with connectivity between the ventral DMN (r6n4) and the right ECN (r3n7). $A\beta_{1-42}$ was positively associated with connectivity between the ventral DMN (r8n4) and the VSN/DAN (r4n8) and negatively associated with connectivity between the ventral DMN (r2n4) and the VSN/DAN (r3n8; Fig. 3A, Table 4).

In the Alzheimer disease group, the functional connectivity of the following networks showed a positive association with CSF total τ levels: the right ECN (r1n7) and the VSN/DAN (r7n8), the left ECN (r1n6) and the right ECN (r3n7), and the VSN/DAN (r2n8) and both the dorsal DMN (r3n3) and the right ECN (r4n7). The $A\beta_{1-42}$ was positively associated with functional connectivity between the ventral DMN (r1n4) and the LN (r5n5) and between the ventral DMN (r3n4) and 2 regions of the anterior SAL (r1n1 and r3n1). The functional connectivity of 2 regions of the LN (r2n5 and r5n5) was positively associated with $A\beta_{1-42}$/phospho-τ (Fig. 3B, Table 4).

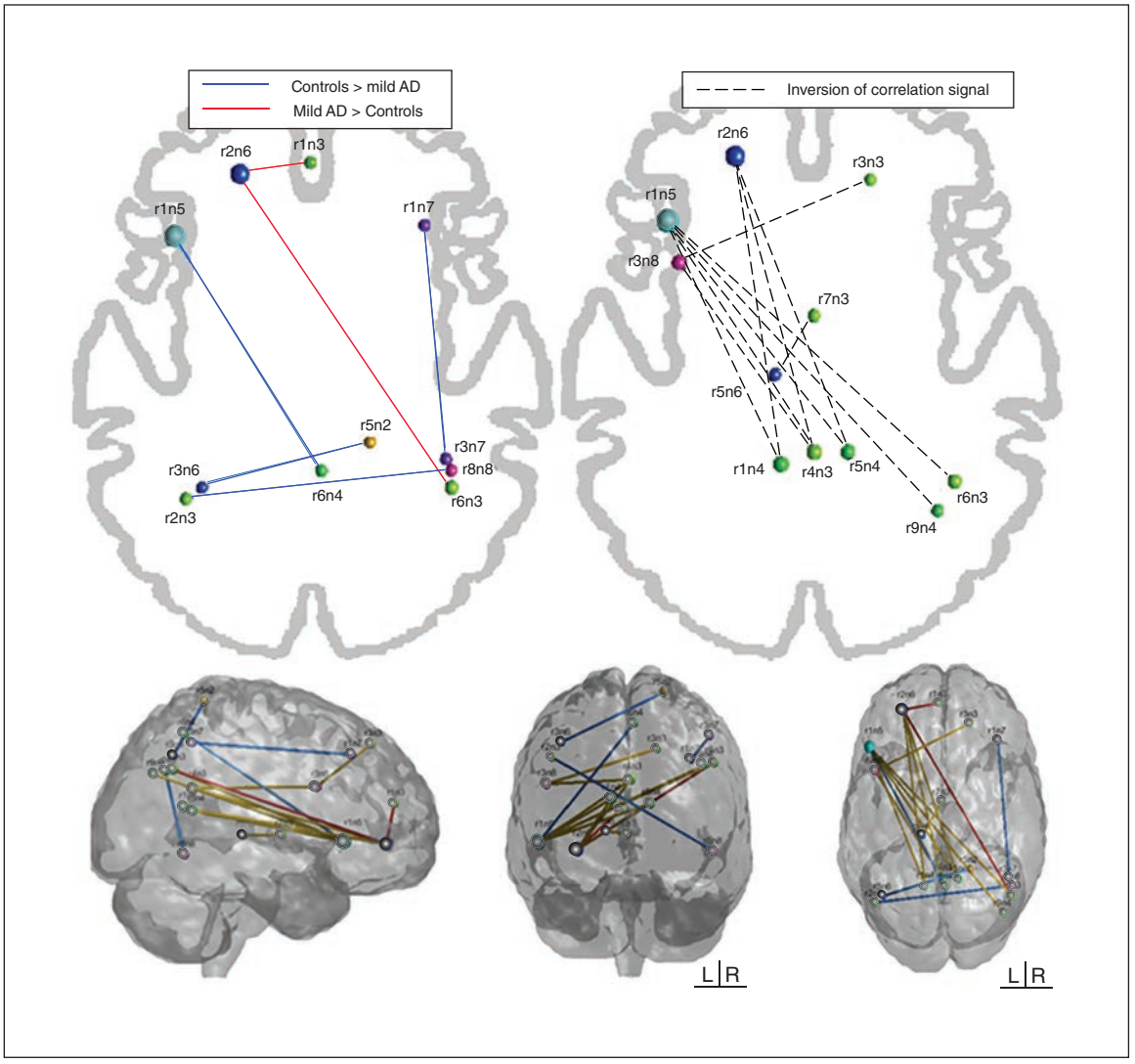

Fig. 2: Region of interest functional connectivity analysis between controls and patients with mild Alzheimer disease (AD). Blue lines represent higher values of functional connectivity in controls, red lines represent higher values in patients with Alzheimer disease (absolute differences in functional connectivity strength between regions of interest), and dashed lines represent an inversion of correlation signal). See Table 1 for anatomic regions.

Table 3: Connections between regions of interest that presented an inversion of the correlation signal in patients with mild Alzheimer disease relative to controls (negative correlation in controls and positive correlation signal in patients with mild Alzheimer disease)

ROI/region	ROI name	Network	Anatomic region
Visuospatial/dorsal attention network (r3n8 — left frontal operculum/inferior frontal gyrus)	r3n3	Dorsal default mode	Right superior frontal gyrus
	r4n3	Dorsal default mode	Posterior cingulate cortex/precuneus
Left executive control network (r2n6 — left inferior frontal gyrus)	r5n4	Ventral default mode	Right retrosplenial cortex/posterior cingulate cortex
	r1n4	Ventral default mode	Left retrosplenial cortex/posterior cingulate cortex
	r4n3	Dorsal default mode	Posterior cingulate cortex/precuneus
Language network (r1n5 — left inferior frontal gyrus)	r1n4	Ventral default mode	Left retrosplenial cortex/posterior cingulate cortex
	r5n4	Ventral default mode	Right retrosplenial cortex/posterior cingulate cortex
	r9n4	Ventral default mode	Right angular gyrus/middle occipital gyrus
	r6n3	Dorsal default mode	Right angular gyrus
	r4n3	Dorsal default mode	Posterior cingulate cortex/precuneus

ROI = region of interest.

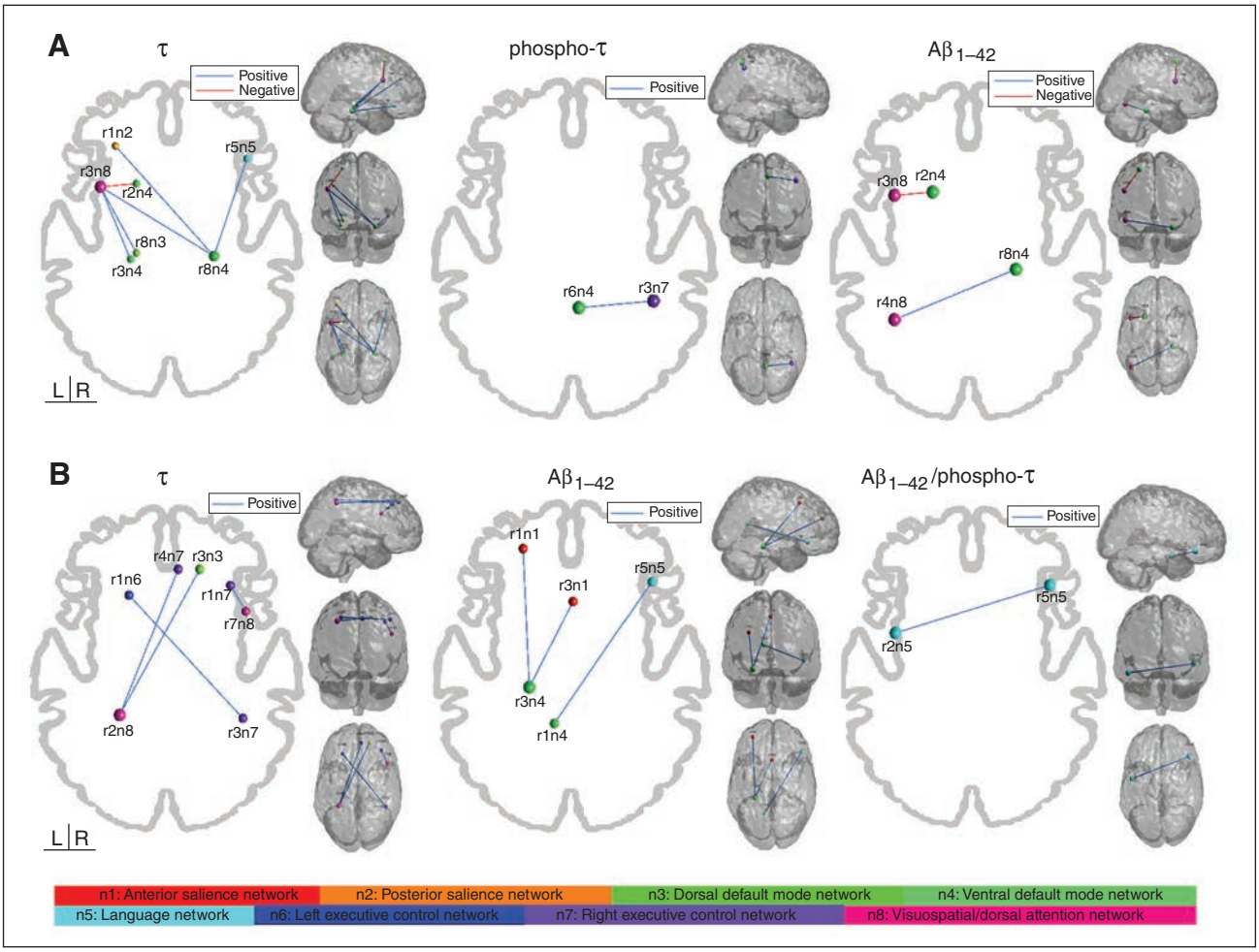

Fig. 3: Significant correlations between functional connectivity in the regions of interest and cerebrospinal fluid (CSF) protein levels in (**A**) patients with amnestic mild cognitive impairment (aMCI) and (**B**) patients with mild Alzheimer disease (AD). Blue lines represent positive correlation, and red lines represent negative correlation. See Table 1 for anatomic regions.

It may be helpful to mention that lower levels of CSF $A\beta_{1–42}$ and $A\beta_{1–42}$/phospho-τ reflect a pattern of Alzheimer disease pathology. A reduced CSF level of $A\beta_{1–42}$ may at least partly be due to a sequestration of amyloid in plaques, with lower levels diffusing to CSF.[21] High levels of CSF total τ and phospho-τ, on the contrary, correlated with the presence of neurofibrillary tangles, predicting the presence of Alzheimer disease pathologic features with high accuracy.[22] In other words, patients with Alzheimer disease are expected to have higher levels of total τ and phospho-τ and lower levels of $A\beta_{1–42}$ and $A\beta_{1–42}$/phospho-τ in the CSF than the healthy elderly population. For patients with aMCI, the higher the CSF total τ and phospho-τ levels (brain pathologic feature), the higher the functional connectivity mainly between the DMN, VSN/DAN and right ECN. On the other hand, a higher level of CSF total τ (brain pathologic feature) was associated with decreased functional connectivity between the VSN/DAN and the DMN. Lower $A\beta_{1–42}$, which reflects higher amyloid burden in the brain (brain pathologic feature), was associated with both stronger and weaker functional connectivity between the VSN/DAN and the ventral DMN.

For patients with Alzheimer disease, the higher the level of CSF total τ, the stronger the functional connectivity of the bilateral ECN, DMN and VSN/DAN. Lower levels of $A\beta_{1–42}$ and $A\beta_{1–42}$/phospho-τ, in turn, were associated with decreased functional connectivity of the anterior SAL, LN and DMN.

Discussion

In the present work, we aimed to evaluate the differences of both intra- and internetwork functional connectivity of large-scale RSNs in the aMCI and Alzheimer disease groups and to correlate the imaging data with characteristic pathophysiological proteins obtained from CSF. Overall, although the DMN was the network with more disruptions in patients with Alzheimer disease, connectivity alterations were not limited to the DMN; other networks were also affected, extending the findings of previous studies. Nearly all RSNs analyzed in the present study were disrupted in patients with Alzheimer disease. Furthermore, these patients presented an inverted correlation (i.e., positive instead of negative) between the DMN and the VSN/DAN, between the DMN and the LN, and between the DMN and the left ECN. Pathological levels of CSF proteins were associated with the connectivity of several RSNs other than the DMN, such as the VSN/DAN, bilateral ECN, anterior SAL and LN, both in patients with aMCI and in those with Alzheimer disease.

Disruptions in RSNs in patients with mild Alzheimer disease have been reported extensively in the literature over the last decade. In the present work, we found that network disruptions in patients with mild Alzheimer disease go beyond intranetwork connectivity, but the associations between RSNs (i.e., internetwork connectivity) are also altered. The Alzheimer disease group showed decreased positive connectivity within the ECN and decreased anticorrelation between the ECN and the posterior SAL. A recent study[23] that used pathophysiological interaction analysis to investigate modulatory interactions among RSNs reported an association between the SAL and executive networks, suggesting that they are functionally connected. Our work in turn, suggests that this connectivity is damaged in patients with Alzheimer disease, aligning with the findings of previous research reporting loss of correlation between the SAL and ECN in patients with Alzheimer disease[5] and even in those with aMCI.[1] Although the present study did not find statistically significant results for the aMCI group, functional connectivity disruptions within[7] and between[1,7] networks in these patients have been reported previously in the literature. Our lack of significant results for patients with aMCI could be due to the heterogeneity of the sample (early v. late aMCI), different cognitive reserve levels, which is known to influence the functional connectivity of networks,[24] or our different methodological approach. The main methodological difference between the present study and previous internetwork functional connectivity studies lies in the analysis of the correlation signal between ROIs. In other words, we did not exclude negative correlations from the analysis (or we used absolute values) to avoid misleading interpretations about the directions of the alterations. By doing so, we could evaluate not only the strength of the correlations, but also their directions.

Among patients with Alzheimer disease, for example, we observed alterations between the DMN and other RSNs, such as a decreased negative connectivity between the ventral DMN and the LN and between the dorsal DMN and the VSN/DAN (which were less anticorrelated in patients with Alzheimer disease), as published previously.[8] On the other hand, we observed an increased correlation between the DMN and the ECN in patients with Alzheimer disease (more positive correlation in Alzheimer disease). Similarly, patterns of inverted correlation were observed between the DMN and

Table 4: Strength of the correlations between cerebrospinal fluid biomarkers and functional connectivity of regions of interest in patients with aMCI and mild Alzheimer disease

Group	CSF biomarker	ROI	ROI	*r*
aMCI	Total τ	r1n2	r8n4	0.63
		r3n8	r2n4	–0.601
		r3n8	r8n3	0.602
		r3n8	r3n4	0.637
		r3n8	r8n4	0.612
		r8n4	r5n5	0.621
	Phospho-τ	r6n4	r3n7	0.55
	$A\beta_{1–42}$	r3n8	r2n4	–0.65
		r4n8	r8n4	0.57
Alzheimer disease	Total τ	r3n3	r2n8	0.698
		r1n7	r7n8	0.769
		r2n8	r4n7	0.697
		r1n6	r3n7	0.765
	$A\beta_{1–42}$	r1n1	r3n4	0.724
		r3n4	r3n1	0.693
		r1n4	r5n5	0.728
	$A\beta_{1–42}$/phospho-τ	r2n5	r5n5	0.693

aMCI = amnestic mild cognitive impairment; CSF = cerebrospinal fluid; ROI = region of interest.

the VSN/DAN, between the DMN and the LN, and between the DMN and the left ECN (anticorrelated in controls and positively correlated in patients with Alzheimer disease).

The complex interactions between the DMN and other networks are of utmost importance for cognitive processing. It is known, for example, that some systems in the brain are intrinsically organized into anticorrelated networks, such as the DMN and external goal-oriented tasks systems.[25] The DMN consists of a set of areas that are suppressed during goal-directed cognition (task-negative network),[26] whereas other RSNs, such as the ECN and VSN/DAN, are recruited in tasks in which participants have to maintain external attention (task-positive networks).[27] Furthermore, decreased suppression of the DMN is associated with poorer cognitive task performance in the healthy population[28] and in cognitive decline groups.[29] Taken together, these findings provide evidence of the complex and intrinsic association between the DMN and task-positive networks for cognition. In the present study, we found that the main connectivity abnormalities in patients with Alzheimer disease occur between the DMN and some task-positive RSNs: not only did patients with Alzheimer disease show less anticorrelation between some regions (between the ventral DMN and the LN, and between the dorsal DMN and the VSN/DAN), but also an inversion of the correlation signal between the DMN and task-positive networks (between the DMN and the VSN/DAN, between the DMN and the LN, and between the DMN and the left ECN, which were positively correlated instead of anticorrelated).

The mechanisms behind this anticorrelation are not yet understood, but it has been suggested that anticorrelated RSNs might have opposed functional roles. For instance, an fMRI study in rats[30] that found anticorrelations within the frontolimbic circuit (between the amygdala and the infralimbic cortex) suggested that their negative association could arise from an inhibitory interaction between these areas. The inversion of the correlation signal found in patients with Alzheimer disease (between regions that would be expected to be anticorrelated) could reflect an inappropriate recruitment of task-positive networks by the DMN to compensate for damage. Furthermore, converging evidence suggests that shifts in excitatory/inhibitory balance in vulnerable cortical circuits are significant drivers in the pathophysiological progression of Alzheimer disease.[31]

Interestingly, most of the correlation abnormalities involved the DMN regions, which are structures known to be hit by the pathophysiological process in Alzheimer disease.[9] For instance, it has repeatedly been demonstrated in PiB-PET studies that the presence of amyloid plaques is sufficient for there to be functional connectivity changes not only in the DMN,[10] but also in the SAL and ECN[32] and even between networks.[33] In the present study, we found that a lower level of CSF $A\beta_{1-42}$ was associated with decreased functional connectivity between the ventral DMN and the LN and between the ventral DMN and the anterior SAL in patients with Alzheimer disease, whereas in patients with aMCI there was stronger functional connectivity between some regions of the ventral DMN and the VSN/DAN and decreased connectivity between other regions of the ventral DMN and the VSN/DAN. Amyloid burden in the DMN areas is a plausible explanation for the functional connectivity disruption between these RSNs; in addition, previous studies using PiB-PET amyloid imaging have demonstrated that amyloid accumulation occurs throughout the lateral frontoparietal cortex[34] and extends to the attention network,[35] affecting the functional connectivity of regions belonging to the VSN/DAN in patients with Alzheimer disease.[36] Furthermore, a lower level of CSF $A\beta_{1-42}$/phospho-τ was associated with decreased functional connectivity within regions of the LN in patients with Alzheimer disease, complementing the results of previous work that found that a lower level of CSF $A\beta_{1-42}$/phospho-τ was associated with DMN disconnectivity.[37]

The extent to which other pathological proteins affect RSN connectivity, however, remains unclear. Among samples obtained from CSF, we showed that besides $A\beta_{1-42}$, total τ and phospho-τ levels also affect the brain's functional connectivity. For instance, both the aMCI and Alzheimer disease groups showed abnormalities in functional connectivity associated with the presence of total τ in the CSF: higher levels of total τ (which reflects neuronal degeneration[38]) in patients with aMCI were associated with disruptions between the DMN and the LN and between the DMN and the VSN/DAN, whereas in patients with Alzheimer disease higher levels of τ were associated with disruptions between the right ECN and the VSN/DAN, between the left and right ECN, between the VSN/DAN and the dorsal DMN, and between the VSN/DAN and the right ECN. Phospho-τ levels also had an impact in patients with aMCI: a higher level of CSF phospho-τ was associated with stronger functional connectivity between the ventral DMN and the right ECN. Although the direction of the association seems unexpected, our results suggest that the presence of a higher level of CSF total τ and phospho-τ implies an imbalance between several brain regions and affects the connectivity of many RSNs, either making them stronger or weaker. In this context, the association between CSF total τ levels and functional alterations in many brain regions should be interpreted in light of the new findings on the spread of the pathological proteins during the course of Alzheimer disease.

Phospho-τ is a protein considered to be an indicator of the pathological hyperphosphorylation process of total τ and the presence of neurofibrillary tangle formation in the brain.[39] Both are concentrated mainly in temporal areas, but various in vitro and in vivo studies have reported the seeding and propagation of total τ aggregates in the brain along the neuroanatomical connections during onset of the disease as well as during its course.[40] Therefore, it is highly likely that the pathological process associated with the τ protein affects the functional communication between brain areas. Furthermore, the tauopathy is highly correlated with cognitive decline and with the clinical progression of Alzheimer disease, suggesting a central role of τ during the course of the disease.[41] In the present work, higher CSF levels of total τ and phospho-τ (i.e., indicators of brain degeneration) were associated with increased functional connectivity between many regions in both patients with aMCI and those with Alzheimer disease that extend beyond the temporal areas.

Limitations

This work has some limitations that must be acknowledged. First, all presented data are cross-sectional, and longitudinal studies would enable investigation of which interactions among RSNs are first disrupted and of possible effects on the connectivity in other RSNs. Second, our findings depend on our choice of seed regions (though our chosen regions had been studied previously[20]), and whole brain functional connectivity analysis or the selection of different ROIs could provide different results. Third, because there was no statistical difference in age among the groups, we decided not to include it as a nuisance variable in our analysis; however, we recognize that aging could be associated with both CSF and functional connectivity results. Regardless of these limitations, the present work provides reliable evidence that the connectivity between several RSNs is disrupted in patients with Alzheimer disease and that CSF protein levels in both patients with aMCI and those with Alzheimer disease are associated with RSN abnormalities.

Conclusion

According to previous studies, the functional alterations in patients with Alzheimer disease extend beyond the connectivity within networks, and the interaction between RSNs are also affected (i.e., internetwork connectivity). We found that the main connectivity abnormalities in patients with Alzheimer disease occur between the DMN and some task-positive RSNs: not only did patients with Alzheimer disease show less anticorrelation between some regions, they also showed an inversion of the correlation signal (positively correlated instead of anticorrelated) between some areas. Abnormal levels of CSF proteins were associated with functional disconnectivity between several regions in both patients with aMCI and those with mild Alzheimer disease, extending well beyond the DMN or temporal areas.

Acknowledgements: The study was supported by the Fundação de Amparo à Pesquisa do Estado de São Paulo grant #2013/10431-9.

Affiliations: From the Neuroimaging Laboratory, University of Campinas, São Paulo, Brazil (Weiler, de Campos, Teixeria, Casseb, Carletti-Cassani, Vicentini, Magalhães, Balthazar); and the Laboratory of Neuroscience, Department & Institute of Psychiatry, Faculty of Medicine, University of São Paulo, São Paulo, Brazil (Talib, Forlenza).

Competing interests: None declared.

Contributors: M. Weiler, B. de Campos and M. Balthazar designed the study. M. Weiler, C. Teixeira, A. Carletti-Cassani, J. Vicentini and T. Magalhães acquired the data, which M. Weiler, B. de Campos, R. Casseb, L. Talib, O. Forlenza and M. Balthazar analyzed. M. Weiler, B. de Campos, R. Casseb, A. Carletti-Cassani, J. Vicentini, T. Magalhães and L. Talib wrote the article, which all authors reviewed and approved for publication.

References

1. He X, Qin W, Liu Y, et al. Abnormal salience network in normal aging and in amnestic mild cognitive impairment and Alzheimer's disease. *Hum Brain Mapp* 2014;35:3446-64.
2. Agosta F, Pievani M, Geroldi C, et al. Resting state fMRI in Alzheimer's disease: beyond the default mode network. *Neurobiol Aging* 2012;33:1564-78.
3. Weiler M, Fukuda A, Massabki LH, et al. Default mode, executive function, and language functional connectivity networks are compromised in mild Alzheimer's disease. *Curr Alzheimer Res* 2014; 11:274-82.
4. Greicius MD, Kimmel DL. Neuroimaging insights into network-based neurodegeneration. *Curr Opin Neurol* 2012;25:727-34.
5. Dai Z, Yan C, Li K, et al. Identifying and mapping connectivity patterns of brain network hubs in Alzheimer's disease. *Cereb Cortex* 2015;25:3723-42.
6. Song J, Qin W, Liu Y, et al. Aberrant functional organization within and between resting-state networks in AD. *PLoS One* 2013; 8:e63727.
7. Wang P, Zhou B, Yao H, et al. Aberrant intra- and inter-network connectivity architectures in Alzheimer's disease and mild cognitive impairment. *Sci Rep* 2015;5:14824.
8. Brier MR, Thomas JB, Snyder AZ, et al. Loss of intranetwork and internetwork resting state functional connections with Alzheimer's disease progression.
9. Buckner RL, Snyder AZ, Shannon BJ, et al. Molecular, structural, and functional characterization of Alzheimer's disease: evidence for a relationship between default activity, amyloid, and memory. *J Neurosci* 2005;25:7709-17.
10. Sheline YI, Raichle ME, Snyder AZ, et al. Amyloid plaques disrupt resting state default mode network connectivity in cognitively normal elderly. *Biol Psychiatry* 2010;67:584-7.
11. McKhann GM. Changing concepts of Alzheimer disease. *JAMA* 2011;305:2458-9.
12. Morris JC. The Clinical Dementia Rating (CDR): current version and scoring rules. *Neurology* 1993;43:2412-4.
13. Albert MS, DeKosky ST, Dickson D, et al. The diagnosis of mild cognitive impairment due to Alzheimer's disease: recommendations from the National Institute on Aging-Alzheimer's Association workgroups on diagnostic guidelines for Alzheimer's disease. *Alzheimers Dement* 2011;7:270-9.
14. Devanand DP, Pradhaban G, Liu X, et al. Hippocampal and entorhinal atrophy in mild cognitive impairment: prediction of Alzheimer disease. *Neurology* 2007;68:828-36.
15. Hachinski VC, Iliff LD, Zilhka E, et al. Cerebral blood flow in dementia. *Arch Neurol* 1975;32:632-7.
16. Fazekas, F, Chawluk, J, Alavi, A, et al. MR signal abnormalities at 1.5 T in Alzheimer's dementia and normal aging. *AJNR Am J Neuroradiol* 1987;149:351-6.
17. Olsson A, Vanderstichele H, Andreasen N, et al. Simultaneous measurement of beta-amyloid(1-42), total tau, and phosphorylated tau (Thr181) in cerebrospinal fluid by the xMAP technology. *Clin Chem* 2005;51:336-45.
18. De Campos BM, Coan AC, Lin Yasuda C, et al. Large-scale brain networks are distinctly affected in right and left mesial temporal lobe epilepsy. *Hum Brain Mapp* 2016;37:3137-52.
19. Van Dijk KR, Sabuncu MR, Buckner RL. The influence of head motion on intrinsic functional connectivity MRI. *Neuroimage* 2012; 59:431-8.
20. Shirer WR, Ryali S, Rykhlevskaia E, et al. Decoding subject-driven cognitive states with whole-brain connectivity patterns. *Cereb Cortex* 2012;22:158-65.
21. Blennow K, Zetterberg H. Cerebrospinal fluid biomarkers for Alzheimer's disease. *J Alzheimers Dis* 2009;18:413-7.
22. Tapiola T, Alafuzoff I, Herukka SK, et al. Cerebrospinal fluid {beta}-amyloid 42 and tau proteins as biomarkers of Alzheimer-type pathologic changes in the brain. *Arch Neurol* 2009;66:382-9.
23. Di X, Biswal BB. Modulatory interactions between the default mode network and task positive networks in resting-state. *PeerJ* 2014; 2:e367.
24. Bozzali M, Dowling C, Serra L, et al. The impact of cognitive reserve on brain functional connectivity in Alzheimer's disease. *J Alzheimers Dis* 2015;44:243-50.
25. Fox MD, Snyder AZ, Vincent JL, et al. The human brain is intrinsically organized into dynamic, anticorrelated functional networks. *Proc Natl Acad Sci U S A* 2005;102:9673-8.
26. Anticevic A, Cole MW, Murray JD, et al. The role of default network deactivation in cognition and disease. *Trends Cogn Sci* 2012; 16:584-92.
27. Cole MW, Schneider W. The cognitive control network: integrated cortical regions with dissociable functions. *Neuroimage* 2007;37: 343-60.

28. Sala-Llonch R, Bosch B, Arenaza-Urquijo EM, et al. Greater default-mode network abnormalities compared to high order visual processing systems in amnestic mild cognitive impairment: an integrated multi-modal MRI study. *J Alzheimers Dis* 2010;22:523-39.
29. Hansen NL, Lauritzen M, Mortensen EL, et al. Subclinical cognitive decline in middle-age is associated with reduced task-induced deactivation of the brain's default mode network. *Hum Brain Mapp* 2014;35:4488-98.
30. Liang Z, King J, Zhang N. Anticorrelated resting-state functional connectivity in awake rat brain. *Neuroimage* 2012;59:1190-9.
31. Kann O. The interneuron energy hypothesis: implications for brain disease. *Neurobiol Dis* 2016;90:75-85.
32. Lim HK, Nebes R, Snitz B, et al. Regional amyloid burden and intrinsic connectivity networks in cognitively normal elderly subjects. *Brain* 2014;137:3327-38.
33. Elman JA, Madison CM, Baker SL, et al. Effects of beta-amyloid on resting state functional connectivity within and between networks reflect known patterns of regional vulnerability. *Cereb Cortex* 2016 ;26:695-707.
34. Sepulcre J, Sabuncu MR, Becker A, et al. In vivo characterization of the early states of the amyloid-beta network. *Brain* 2013;136:2239-52.
35. Myers N, Pasquini L, Gottler J, et al. Within-patient correspondence of amyloid-beta and intrinsic network connectivity in Alzheimer's disease. *Brain* 2014;37:3137-52.
36. Koch K, Myers NE, Gottler J, et al. Disrupted intrinsic networks link amyloid-beta pathology and impaired cognition in prodromal Alzheimer's disease. *Cereb Cortex* 2015.
37. Li X, Li TQ, Andreasen N, et al. Ratio of Abeta42/P-tau181p in CSF is associated with aberrant default mode network in AD. *Sci Rep* 2013;3:1339.
38. Andreasen N, Vanmechelen E, Vanderstichele H, et al. Cerebrospinal fluid levels of total-tau, phospho-tau and A beta 42 predicts development of Alzheimer's disease in patients with mild cognitive impairment. *Acta Neurol Scand Suppl* 2003;179:47-51.
39. Buerger K, Ewers M, Pirttila T, et al. CSF phosphorylated tau protein correlates with neocortical neurofibrillary pathology in Alzheimer's disease. *Brain* 2006;129:3035-41.
40. Walker LC, Diamond MI, Duff KE, et al. Mechanisms of protein seeding in neurodegenerative diseases. *JAMA Neurol* 2013;70:304-10.
41. Han SD, Gruhl J, Beckett L, et al. Beta amyloid, tau, neuroimaging, and cognition: sequence modeling of biomarkers for Alzheimer's disease. *Brain Imaging Behav* 2012;6:610-20.